PLANETARY NEBULAE IN M82: KINEMATIC AND PHOTOMETRIC ANALYSIS

L.C. Johnson (Colby College & Institute for Astronomy, University of Hawaii), R. H. Méndez & A.M. Teodorescu (Institute for Astronomy, University of Hawaii)

Abstract

Using an on-band/off-band filter technique, we identify 114 planetary nebulae (PNe) in the edge-on spiral galaxy M82 using the FOCAS instrument at the 8.2m Subaru Telescope. Radial velocities were determined for 100 of these PNe using a method of slitless spectroscopy, from which we obtain a clear picture of the galaxy's rotation. We find evidence for a Keplerian decline in M82's rotation curve, in agreement with results derived by CO(2-1) and HI measurements. These results affirm the use of PN as effective, accurate kinematic probes of galaxies. [OIII] emission line photometry of the PNe yielded the planetary nebula luminosity function (PNLF) for the galaxy, allowing us to derive a distance measurement. We confirmed the validity of our PN identifications, and thus the legitimacy of our PNLF using Hα photometry from the ACS instrument on the Hubble Space Telescope. Our distance determination is consistent with other measurements made of the M81/M82 group using Cepheid variable stars and the tip of the red giant branch (TRGB) technique. This work was conducted in a Research Experience for Undergraduates (REU) position at the University of Hawaii's Institute for Astronomy and funded by the NSF.
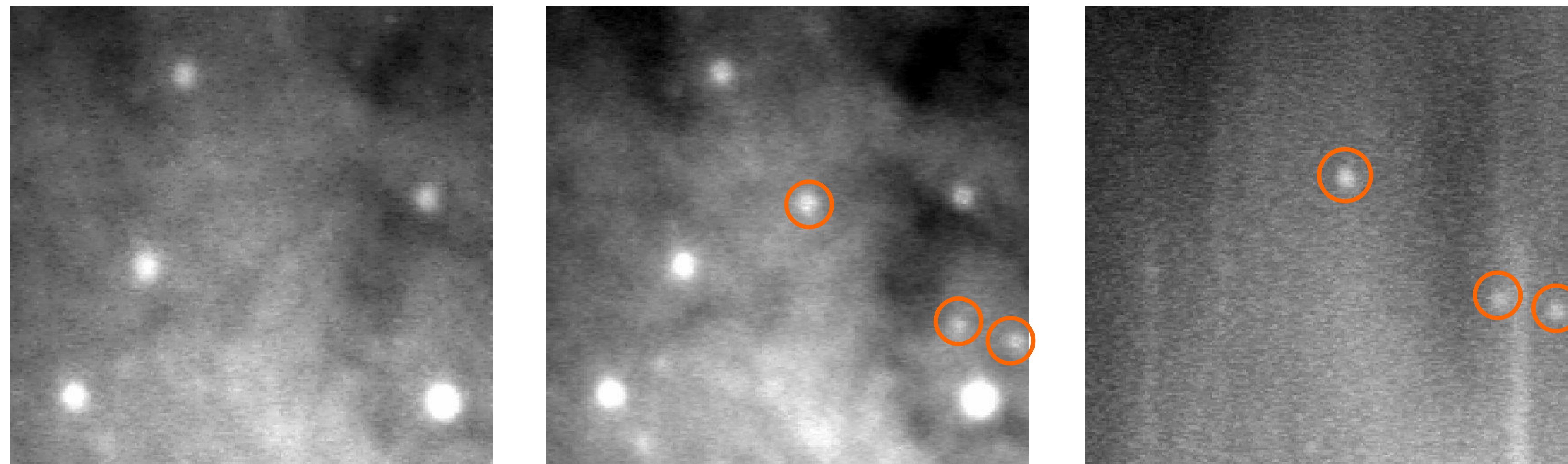
Fig 1. Off-band (left panel), on-band (center panel), and grism (right panel) image sections. Notice 3 PN objects (circled) are visible in the on-band and grism images, but not in the off-band image. Also notice the upward shift in the locations of the sources that occurs between the on-band and grism images.

PN Detection and Slitless Spectroscopy

- PNe have a strong spectral emission feature at 5007 Å.
- Observations are conducted using three image types: on-band (narrowband filter centered on emission feature), off-band (broadband filter), and grism (a dispersed on-band image).
- PNe can be identified by their point source detection in on-band and grism images and their non-detection in an off-band image.
- When the grism is inserted, sources are shifted in the image according to wavelength and location on CCD chip.
- The system can be calibrated in order to determine the relationship between shift and wavelength as a function of chip location. Once calibrated, wavelength and thus radial velocity can be derived for each PN object

NASA, ESA, C.R. O'Dell, M. Meixner and P. McCullough

Fig 2. A planetary nebula – NGC 7293

Fig 3. (Left) A plot of filter transmissions comparing narrowband and broadband filters. The position of 5007Å is marked by black line.

Fig 4. (Right) The spectra of NGC 7293 showing distinctive PN emission lines. Note that the [OIII] emission line is more powerful than the Hα emission line (Henry, et al. 2004).
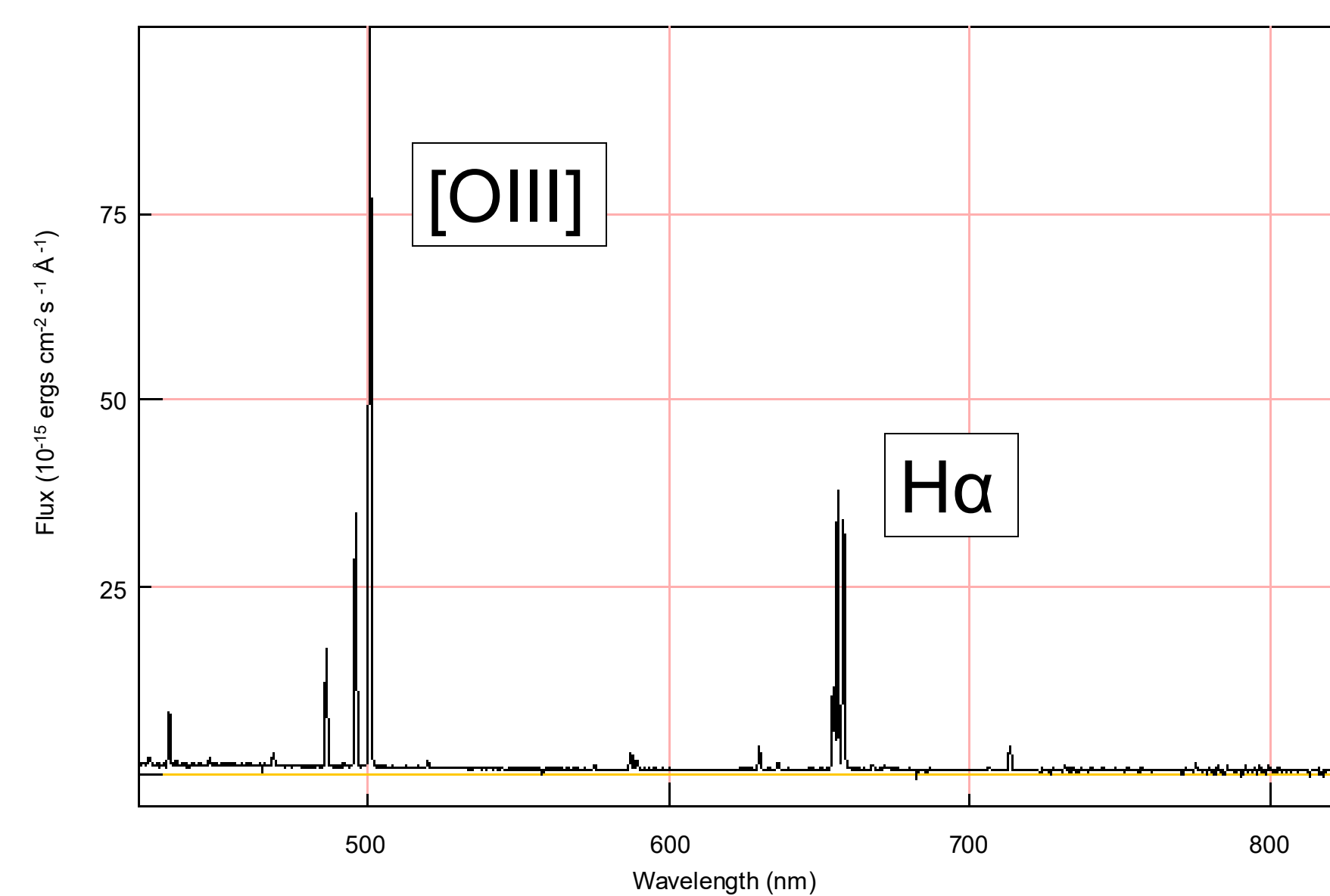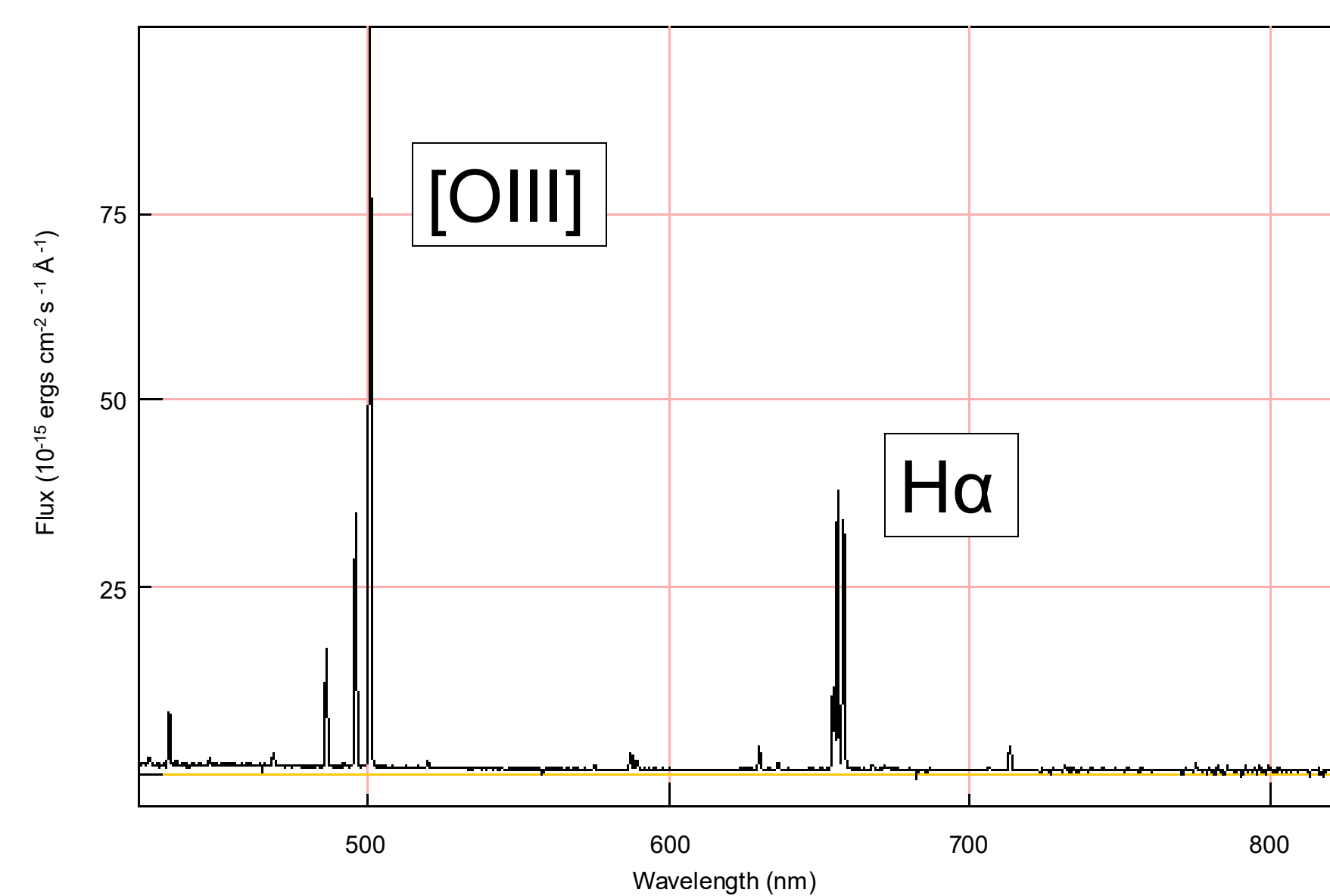
References

Achtermann, J.M., & Lacy, J.H. 1995, ApJ, 439, 163
Feldmeier, J.J., et al. 1997, ApJ, 479, 231
Henry, R.B.C., et al. 2004, AJ, 127, 2284
Mayya, Y.D., et al. 2005, ApJL, 628, L33
McKeith, C.D. et al. 1993, A&A, 272, 98

Méndez, R.H. et al. 2001, ApJ, 563, 135
Puxley, P.J. 1991, MNRAS, 249, 11
Sakai, S., & Madore, B.F. 1999, ApJ, 526, 599
Sofue, Y. 1998, PASJ, 50, 227
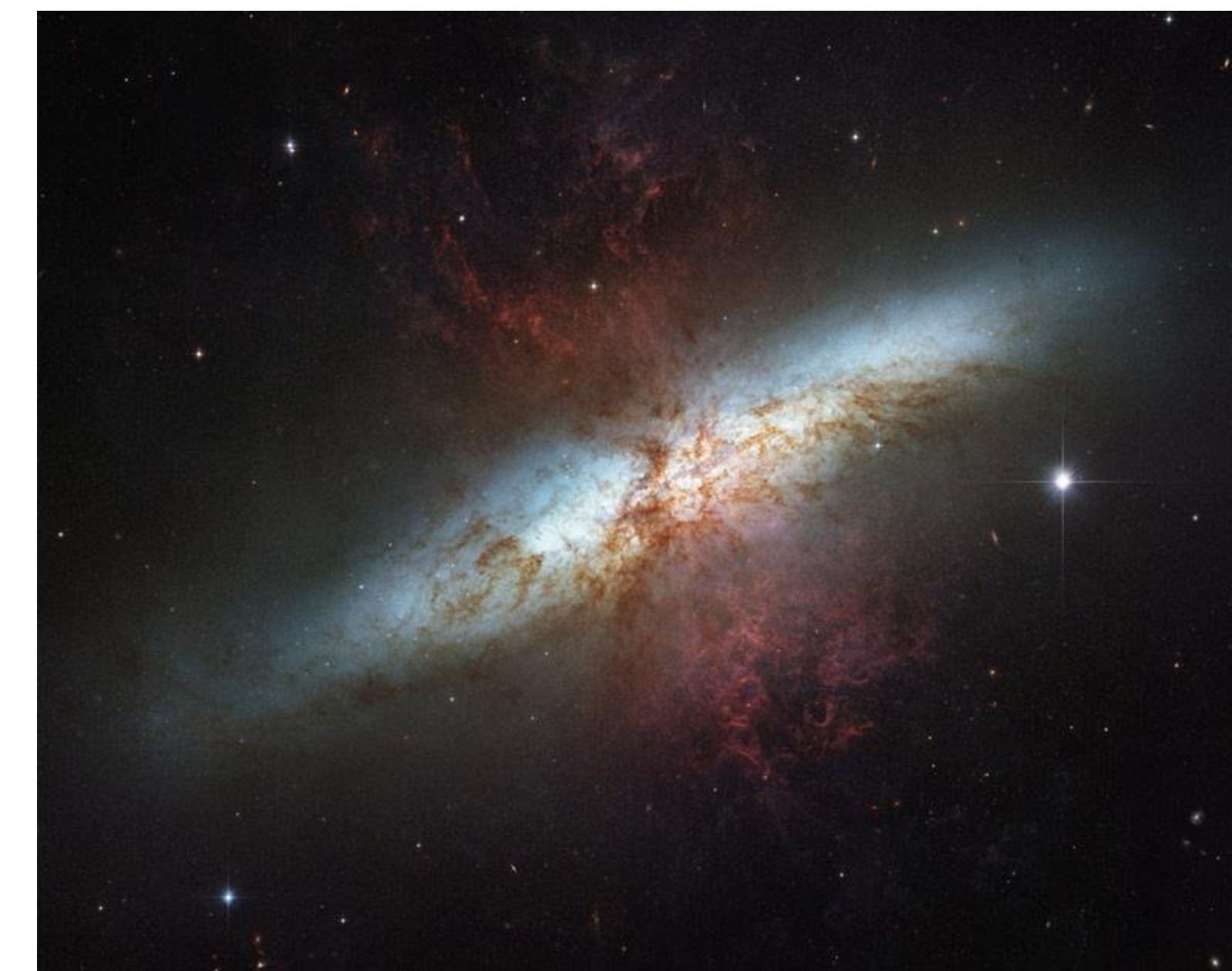Teodorescu, A.M. et al. 2005, ApJ, 635, 290

NASA, ESA, and The Hubble Heritage Team (STScI/AURA)

Fig 5. HST combined image of M82.

Observations and Results

- [OIII] and V imaging and spectroscopy with FOCAS instrument on 8.2 m Subaru Telescope, Mauna Kea, Hawaii
- Hα, B, V, I imaging with ACS instrument onboard the Hubble Space Telescope

- Identified 115 PN candidate objects
- Measured velocities of 100 PN candidate objects ranging from -18 to 393 km s^{-1} ($\pm$10 km s^{-1})
- Performed [OIII] photometry on 110 PN candidate objects.
- Performed Hα photometry on candidates in order to determine their λ5007-to-Hα emission line ratios. We expect PNe to have a ratio greater than 2, while HII regions that may try to containment our sample generally have lower emission line ratios.
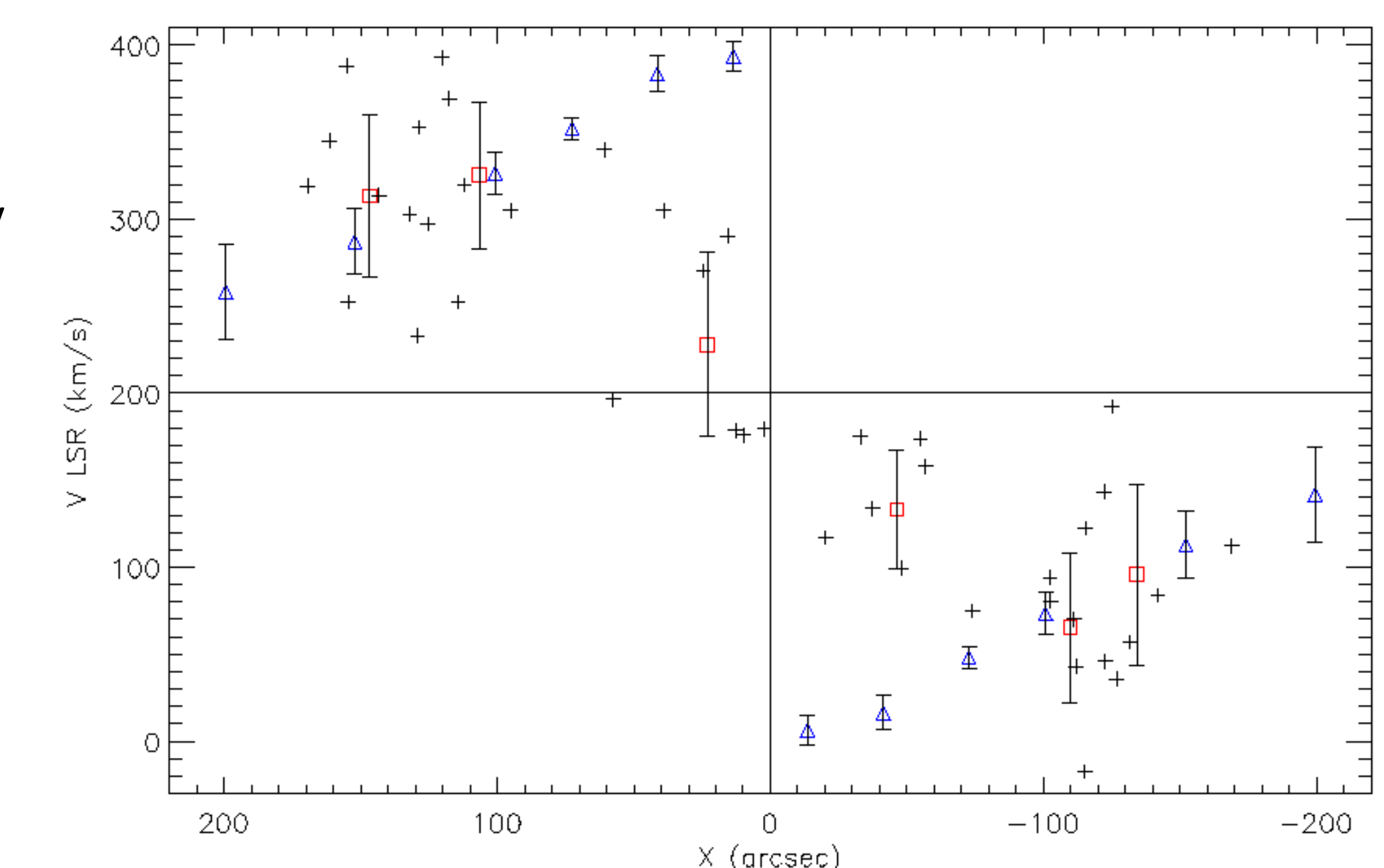
Kinematic Analysis

- Velocity data from 100 PN objects shows agreement with systemic velocity of 200 km s^{-1} (Achtermann & Lacy 1995; McKeith et al. 1993) and basic kinematics of system, where the southwest side of disk (negative major axis offset) is approaching, northeast side (positive major axis offset) is receding (Mayya et al. 2005; Sofue 1998 and others).

- Outside a region of $\pm$70"from the galactic center along major axis, velocity data from PN objects that lie near or within the disk show agreement with a proposed Keplerian decline in rotational velocity found in CO(2-1) and HI observations (Sofue 1998).

- Disagreement of our velocity data within $\pm$70"of the center is due to optical extinction estimated to be A$_v$=27 (Puxley 1991). In this nearly edge-on system, high-velocity PNe that lie near the center of the disk cannot be detected through many magnitudes of extinction, thus only allowing us to detect low-velocity PNe that lie near the edge of the disk.

Fig 6. A plot of major axis position versus radial velocity for 42 PNe within minor axis offset of ±0.5 kpc (≈27"). Red boxes with bars represent binned velocities and the dispersion within those measurements. Blue triangles mark CO rotation curve from Sofue (1998). Individual data points are shown as plus signs.

Photometric Analysis

- On the size scale of galaxies, there is a standard distribution of [OIII] luminosities among a population of PNe.

- When this standard luminosity function is know, we can fit it to an observed population using the bright end of PNLF, where the number of sources falls off at a maximum luminosity.

- The apparent magnitude where this fall off occurs is a function of the distance to the population, thus measuring the PNLF allows for an accurate distance measurement to the system. There are numerious examples of successful applications of this method of distance determination (eg – Feldmeier, Ciardullo, & Jacoby 1997)

- Our preliminary findings show good agreement with literature values for a distance to M82 of 3.9 Mpc (Sakai & Madore 1999).
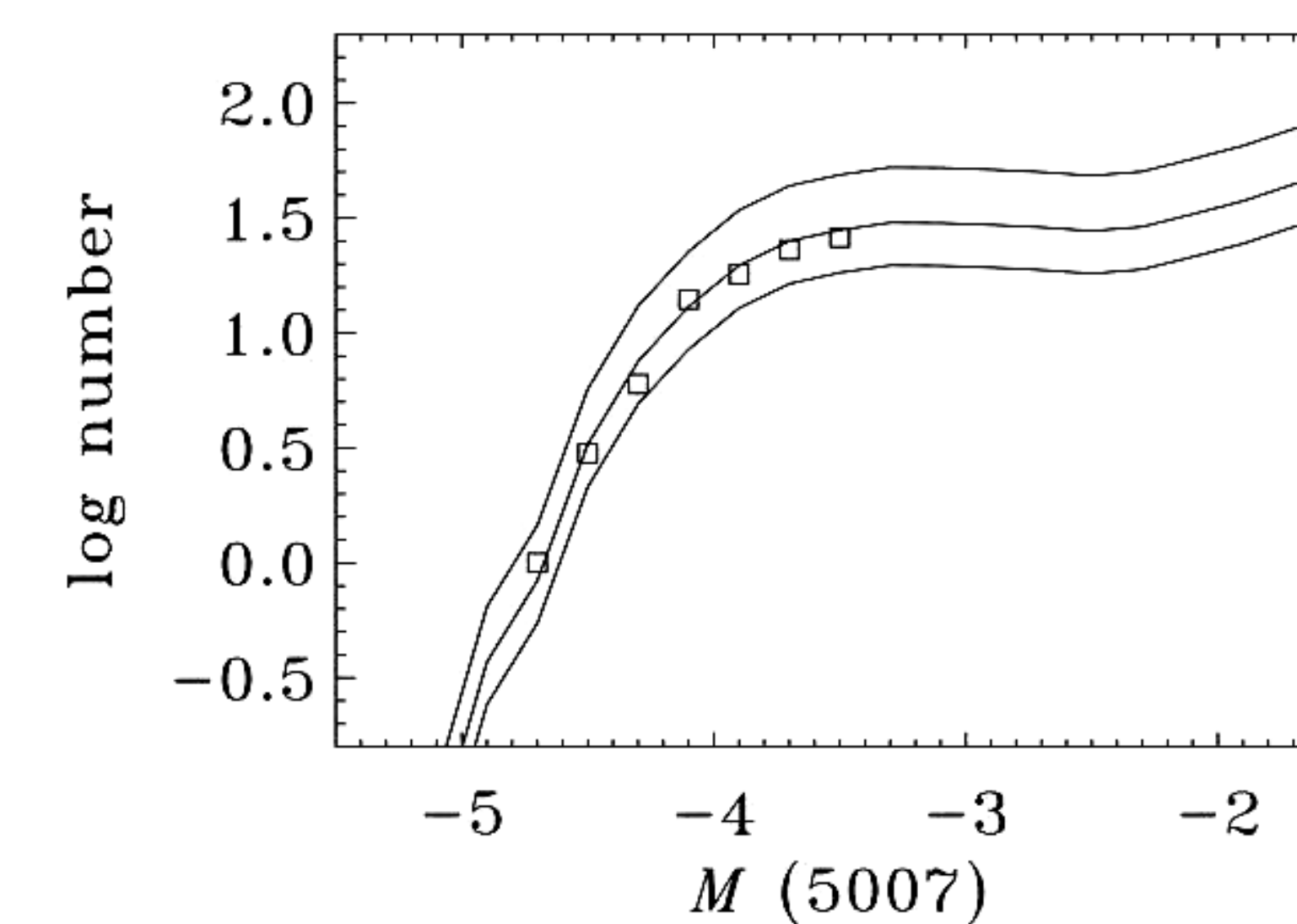

Fig 7. An example of a PNLF.